Electronic Supplementary Material (ESI) for Journal of Materials Chemistry A.

SUPPLEMENTARY INFORMATION

FOR

Nanocatalysts for hydrogen production from borohydride hydrolysis: graphene-derived thin films with Ag and Ni-based nanoparticles

Leandro Hostert, Eduardo G. C. Neiva, Aldo J. G. Zarbin and Elisa S. Orth*

Department of Chemistry, Universidade Federal do Paraná PR), CP 19032, CEP 81531-980 Curitiba Brazil.

1. CHARACTERIZATION of rGO/Ni

The Raman spectra of the rGO/Ni, rGO and GO are in Fig. S1. It's possible to infer the intensification in the D band after the reduction of GO, which accounted for all samples but no more significant differences were observed between them.

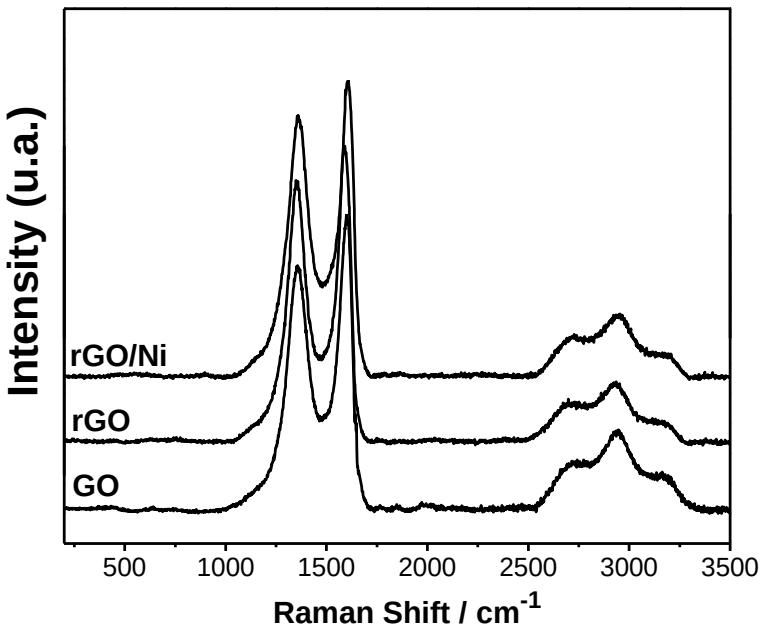

Fig. S1 Raman spectra of rGO/Ni, rGO and GO. The Raman spectra were recorded using a laser of λ = 514.5 nm.

The TGA analysis for rGO/Ni, GO and rGO are illustrated in Fig. S2, for the nanocomposite it was not possible to quantify the percentage of groups oxidized as seen for GO, since the presence of the nickel catalyzes the oxidation of carbon dioxide, causing the events attributed to the elimination of these overlap to the oxidation of the carbonic structure of rGO. The value of metallic nickel percentage was 46.9%, being that above of 470 °C there is a

mass gain due to the oxidation of nickel (Table S1). There is also a decrease in stability of the carbonic structure with the presence of nickel in the samples, as previously reported. This phenomenon is related to catalysis promoted by the metallic particles.[1,2]

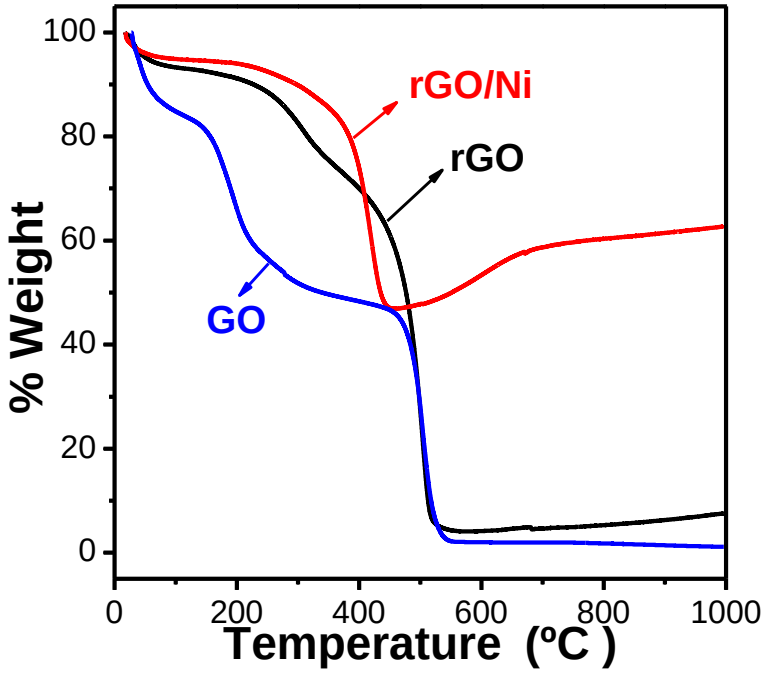

Fig. S2 TGA curves of rGONi, rGO and GO. The TGA analyzes were carried out in a synthetic air atmosphere with a heating rate of 5 °C min^{-1}.

Table S1. Percentages of mass loss (TGA) of the samples: rGO/Ni, rGO and GO.

	Water	Oxygenated groups%	Carbon%	Ni%	NiO%
rGO/Ni	5.3	----	47.8	46.9	62.6
rGO	7	19.5	68.6	----	----
GO	15.9	36.6	45.5	----	----

If compared the TGA of rGO/Ni with rGO/$Ni(OH)_2$ reported by our group[3] both presented a decreased in the thermal stability of carbon structured and the percentage of NiO is higher for rGO/Ni (62.6%) if compared to rGO/$Ni(OH)_2$ (45.5%). The event of loss of mass (130 to 480 °C) for rGO/$Ni(OH)_2$ does not refer only to carbon oxidation, but elimination of ethylene glycol which is acting as a passivate of nanoparticles, and the decomposition of $Ni(OH)_2$ hydroxyls in nanocomposites, leading to NiO. [163] Another relevant information is the difference in percentage of H_2O loss (T_{amb}-190 °C), which was higher for $Ni(OH)_2$ (11.5%) than rGO/Ni (5.3%). The higher amount of H_2O present in nanocomposites corroborates the XRD data related to the higher lamellae distance for $Ni(OH)_2$ obtained in this material, which leads to a greater intercalation of H_2O.

The SEM images (Fig S3) for rGO/Ni is distinguished by the presence of a large amount of particles decorating the graphene sheets, where these

particles have size up to 5 μm. But the surface of these particles presented an irregular surface containing small pores, suggesting that they may have been formed by coalescing (secondary growth) and/or particle aggregation as can be seen in Fig S3 (A, B, C and D). The EDS mapping was carried out in the region illustrated in Fig S3 (E) and it's possible to confirm that the microparticles presented in the film are formed by Ni structured.

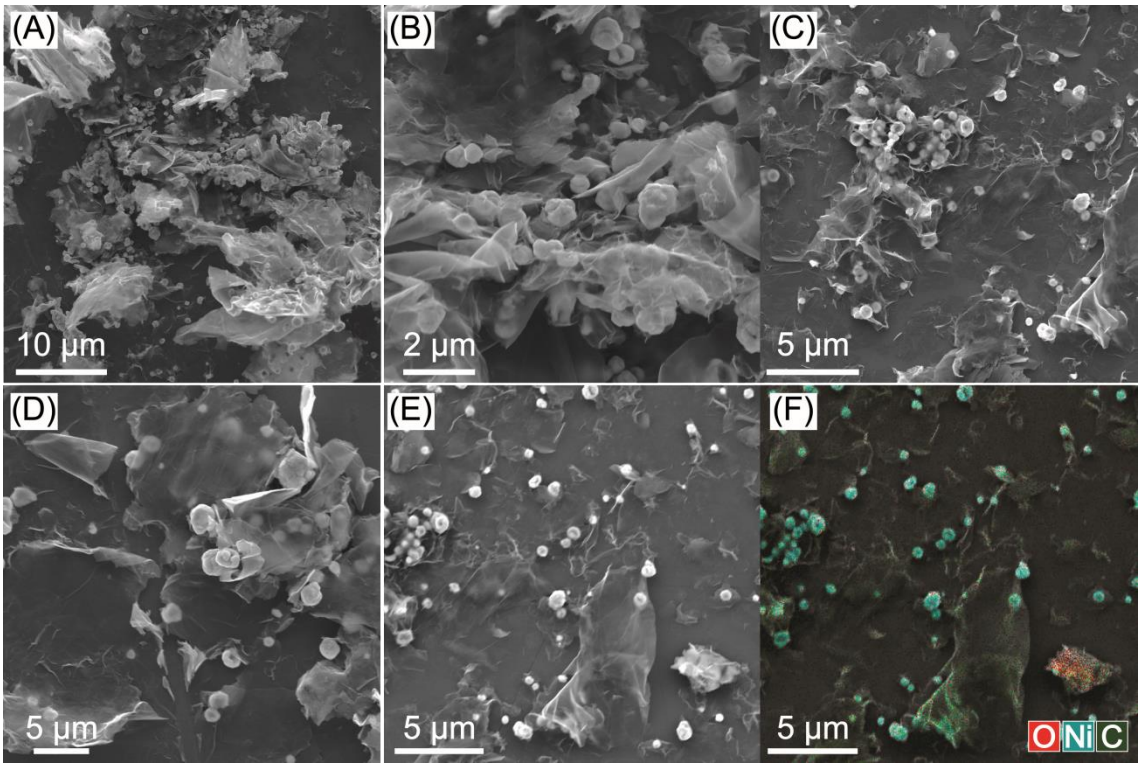

Fig. S3 (A), (B), (C), (D) and (E) SEM images of rGONi using secondary electron detector. (F) Mapping by EDS of the image (E). Using a MIRA-3 FEG-SEM Tescan with 10 kV voltage and a secondary electrons detector.

2 CHARACTERIZATION OF THE NANOCOMPOSITES DURING THE H_2 PRODUCTION REACTION

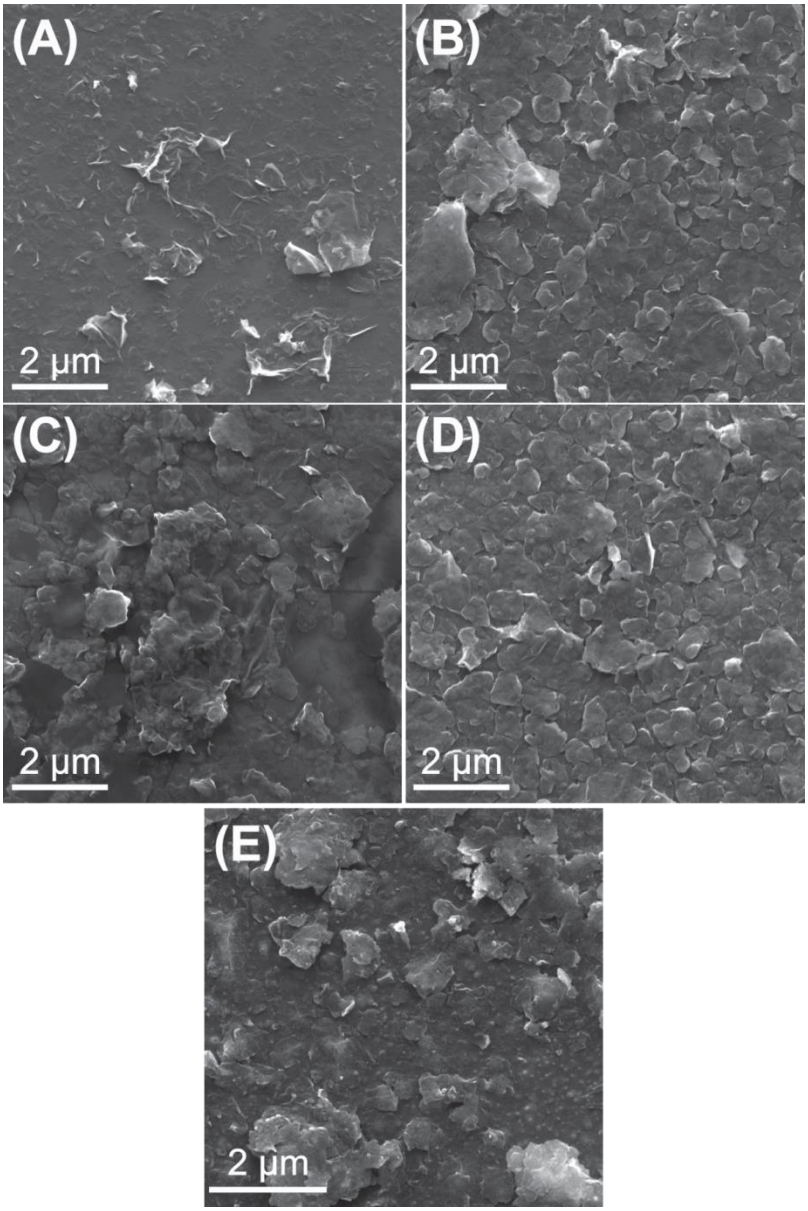

Fig. S4 SEM illustrations of rGO/$Ni(OH)_2$. (A) Before use; (B) 1h; (C) 3h; (D) 6h and (E) 12h of use. Thin film deposited over Si/SiO_2. Using a MIRA-3 FEG-SEM Tescan with 10 kV voltage and a secondary electrons detector.

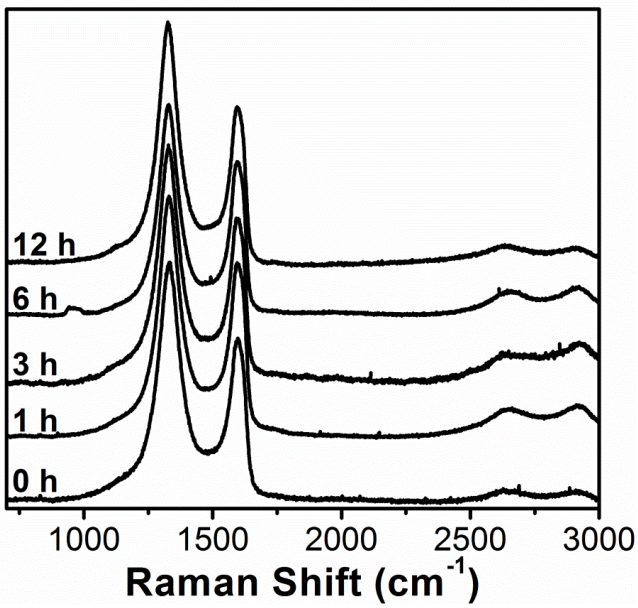

Fig. S5 Raman spectra of rGO/Ni(OH)$_2$ in different times of reaction. Thin film deposited on Si/SiO$_2$ and λ = 632,8 nm.

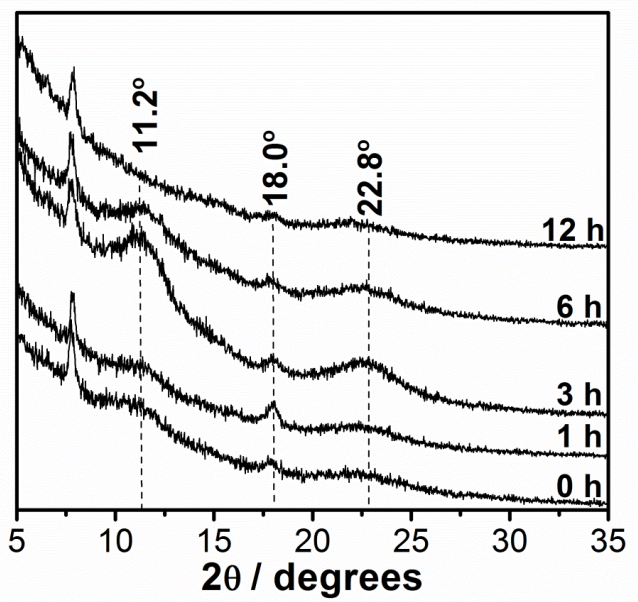

Fig. S6 XRD patterns of rGO/Ni(OH)$_2$ in different times of reaction. The thin films were analyzed using a low angle accessory with 0.1° incident angle operating at 40 kV and 40 mA.

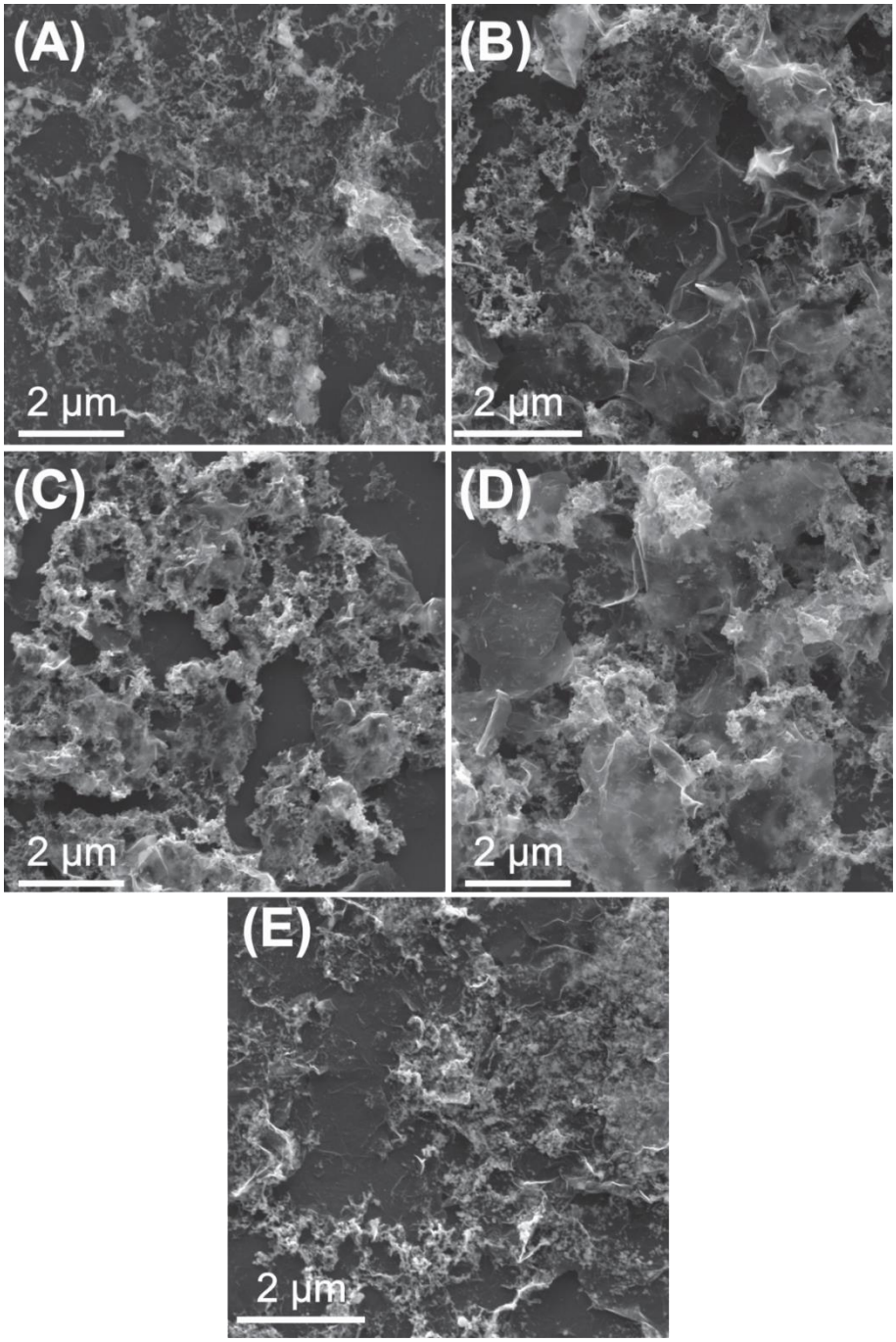

Fig. S7 SEM illustrations of rGO1/Ag. (A) Before use; (B) 1h; (C) 3h; (D) 6h and (E) 12h of use. Thin film deposited over Si/SiO_2. Using a MIRA-3 FEG-SEM Tescan with 10 kV voltage and a secondary electrons detector.

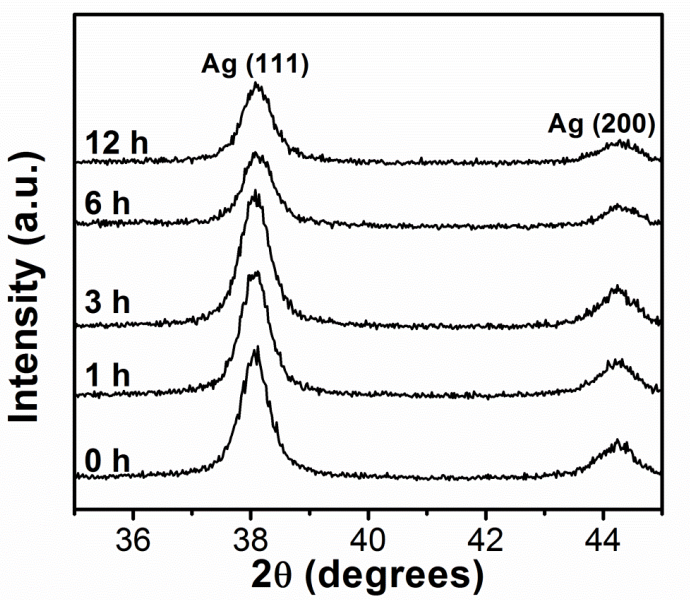

Fig. S8 XRD patterns of rGO1/Ag in different times of reaction. The thin films were analyzed using a low angle accessory with 0.1° incident angle operating at 40 kV and 40 mA.

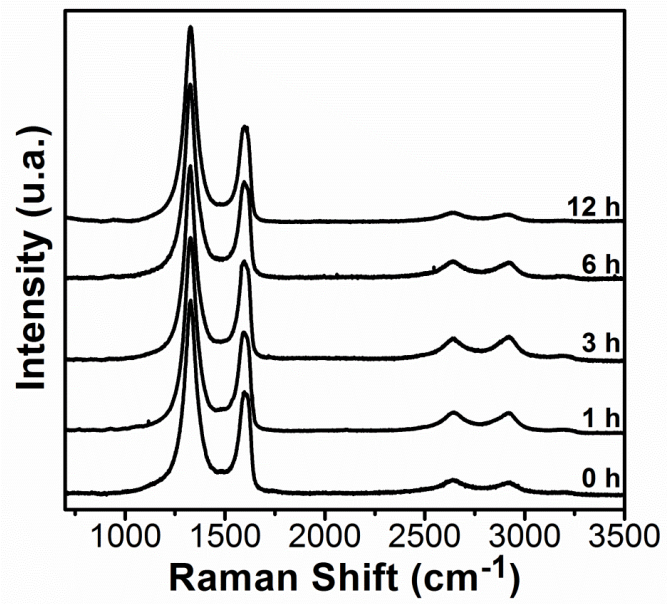

Fig. S9 Raman spectra of rGO1/Ag in different times of reaction. Thin film deposited on Si/SiO_2 and λ = 632,8 nm.

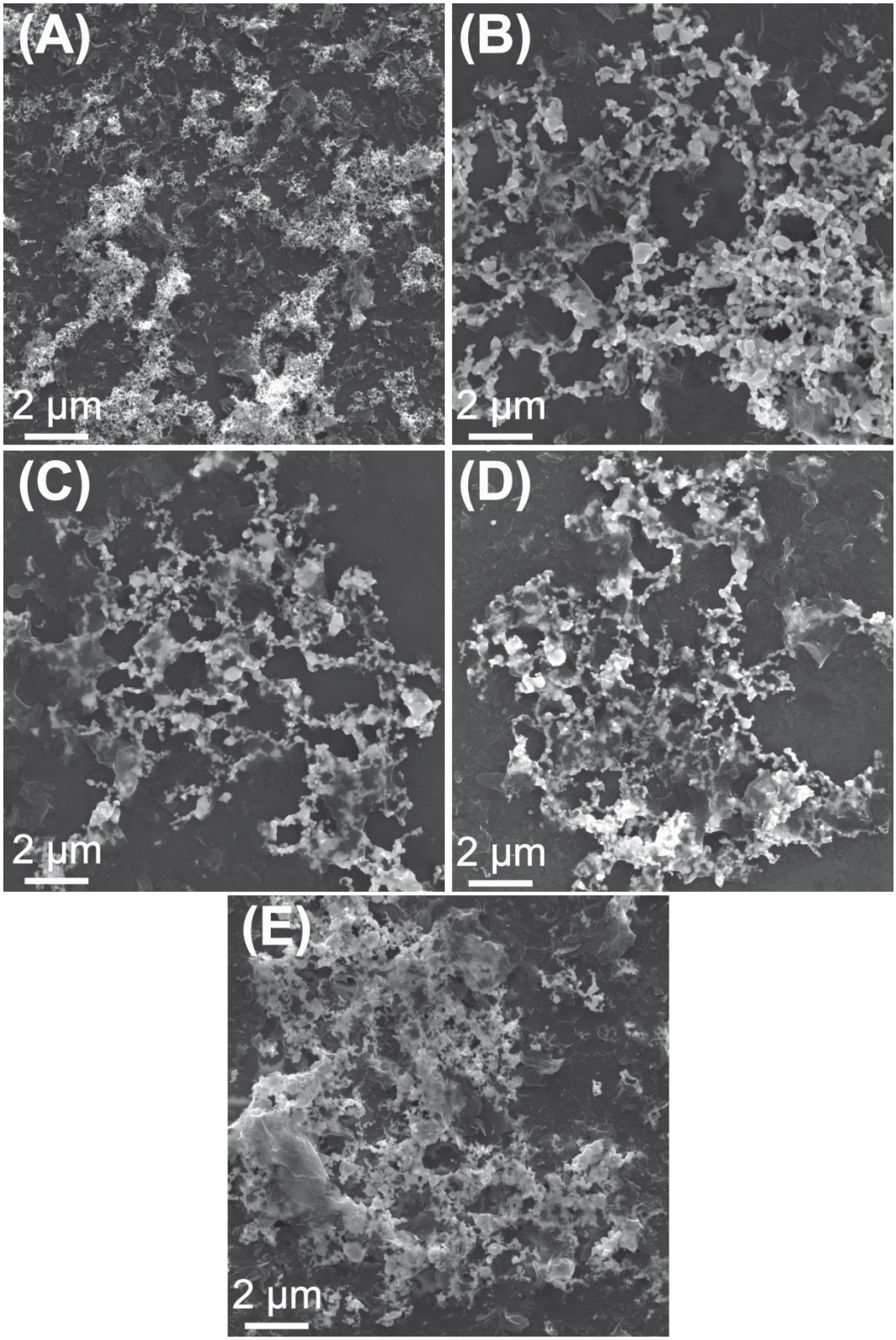

Fig. S10 SEM illustrations of rGO2/Ag. (A) Before use; (B) 1h; (C) 3h; (D) 6h and (E) 12h of use. Thin film deposited over Si/SiO_2. Using a MIRA-3 FEG-SEM Tescan with 10 kV voltage and a secondary electrons detector.

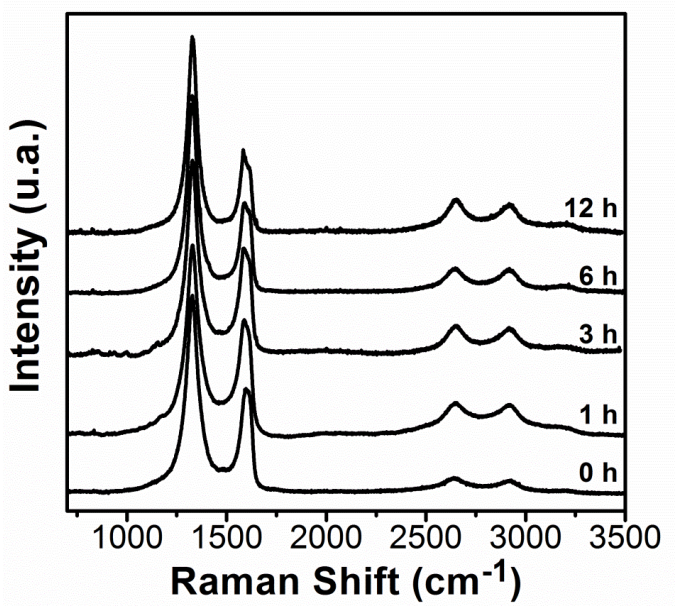

Fig. S11 Raman spectra of rGO2/Ag in different times of reaction. Thin film deposited on Si/SiO_2 and λ = 632,8 nm.

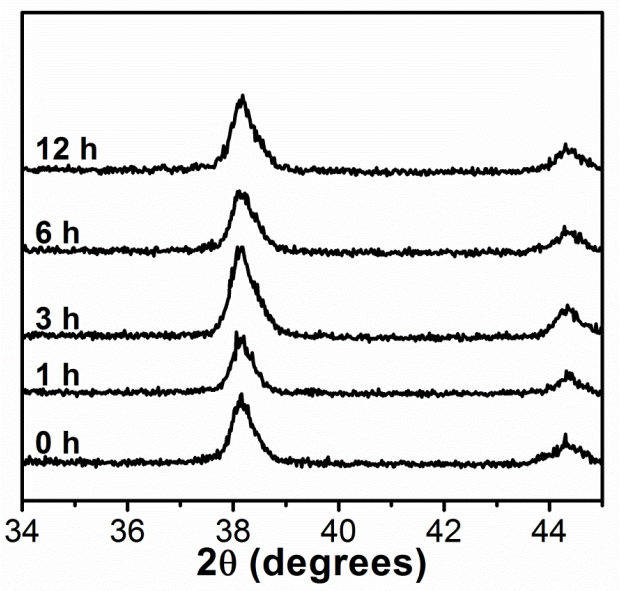

Fig. S12 XRD patterns of rGO2/Ag in different times of reaction. The thin films were analyzed using a low angle accessory with 0.1° incident angle operating at 40 kV and 40 mA.

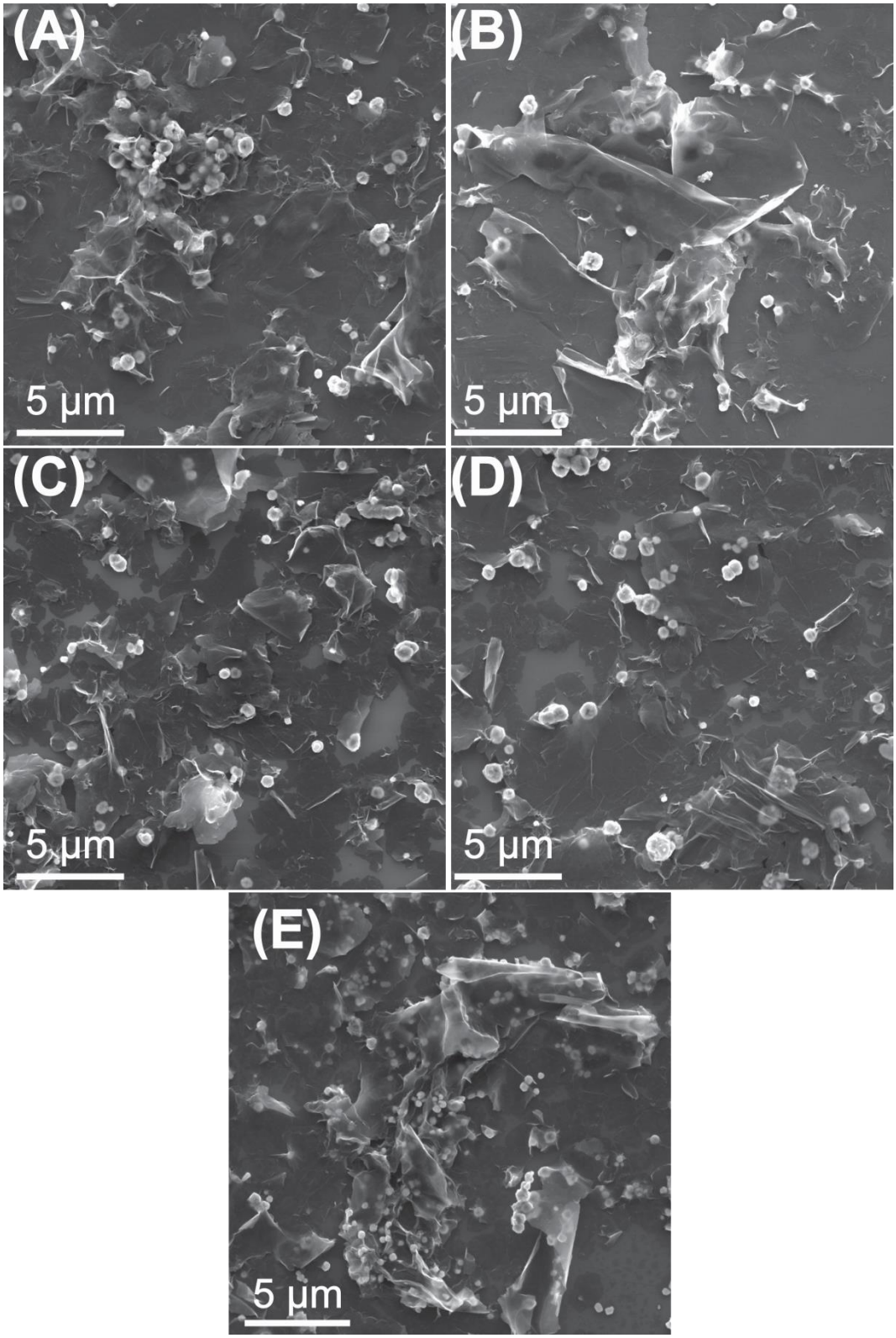

Fig. S13 SEM illustrations of rGO/Ni. (A) Before use; (B) 1h; (C) 3h; (D) 6h and (E) 12h of use. Thin film deposited over Si/SiO_2. Using a MIRA-3 FEG-SEM Tescan with 10 kV voltage and a secondary electrons detector.

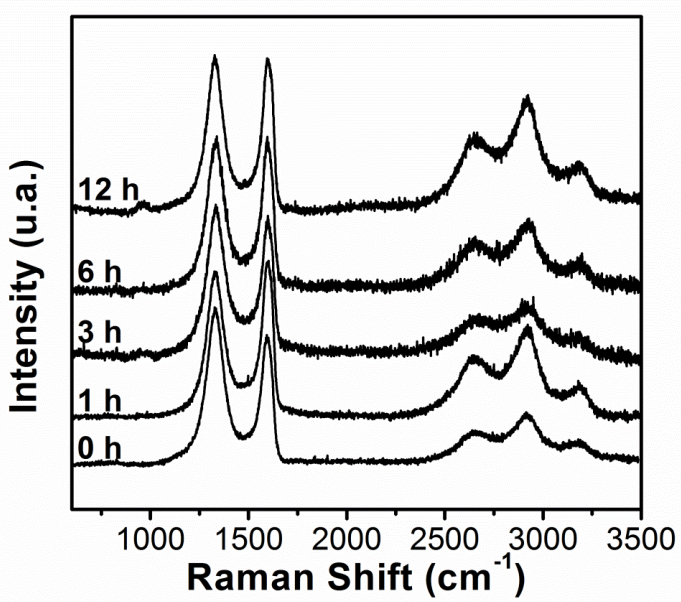

Fig. S14 Raman spectra of rGO/Ni in different times of reaction. Thin film deposited on Si/SiO_2 and λ = 632,8 nm.

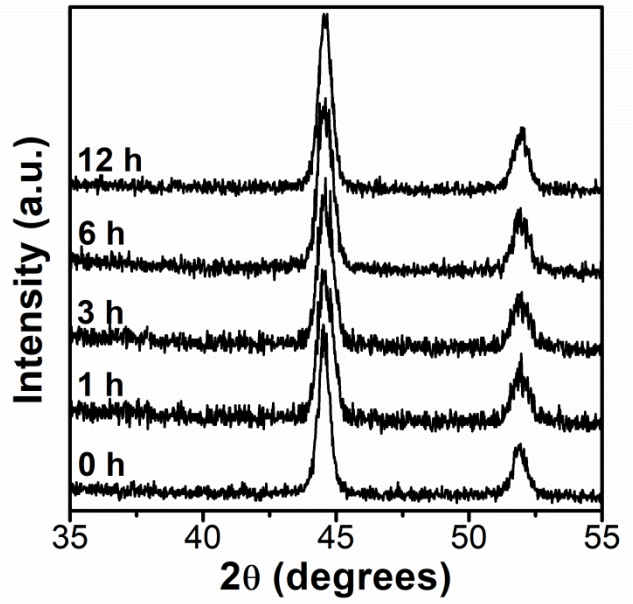

Fig. S15 XRD patterns of rGO/Ni in different times of reaction. The thin films were analyzed using a low angle accessory with 0.1° incident angle operating at 40 kV and 40 mA.

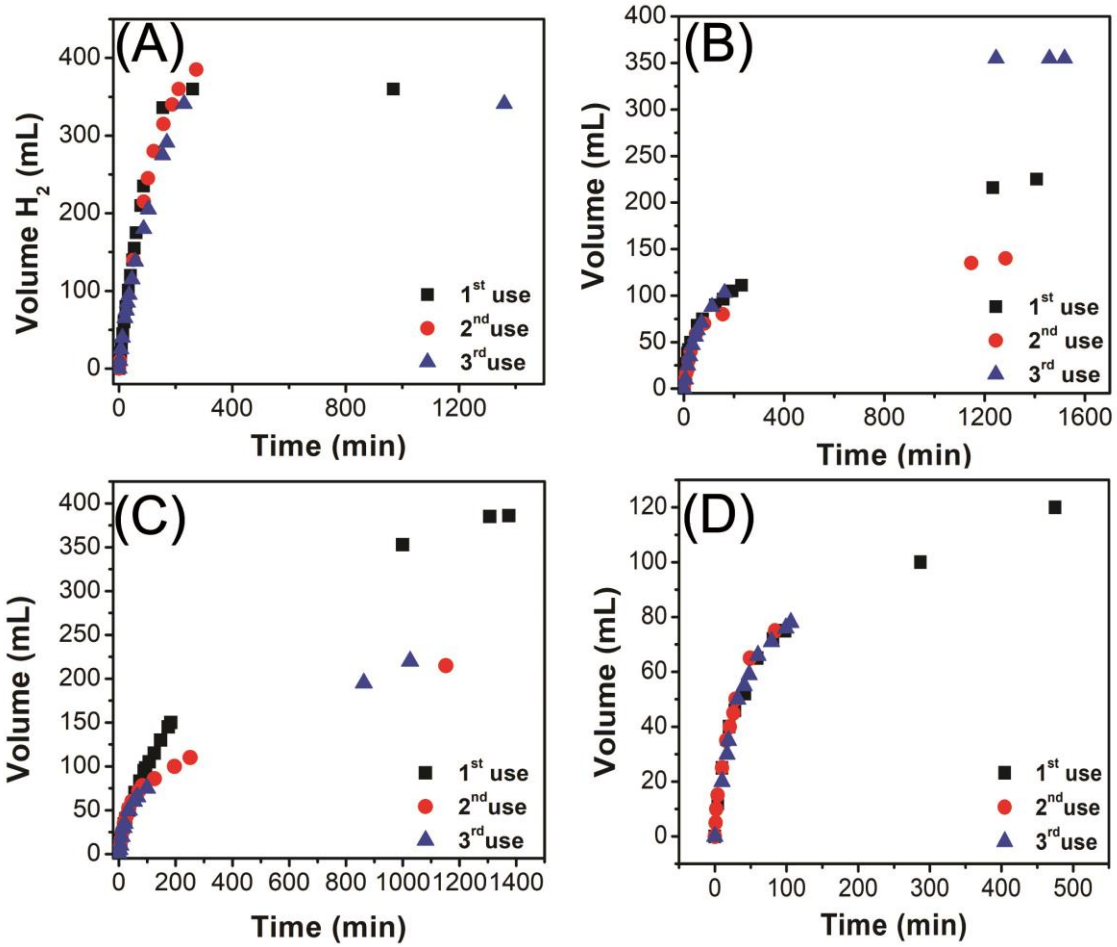

Fig. S16 Recycle study with the 4 nanocomposites used in the work. (A) rGO/Ni; (B) rGO/Ni$(OH)_2$; (C) rGO1/Ag; (D) rGO2/Ag.

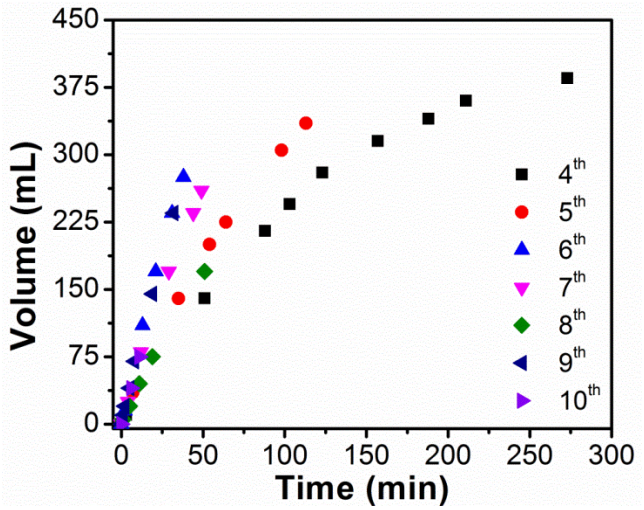

Fig. S17 Consecutive recycles study with rGO/Ni nanocomposite used in the work.

REFERENCES

[1] Mehl, H., Oliveira, M. M., Zarbin, A. J. G. Journal of Colloid and Interface Science, 2015, **438**, 29-38,.

[2] Faria, A. F., Martinez, D. S. T., Meira, S. M. M., De Moraes, A. C. M., Brandelli, A., Filho, A. G. S., Alves, O. L. Colloids and Surfaces B: Biointerfaces, 2014, **113**, 115-124.

[3] E. G. C. Neiva, M. M. Oliveira, M. F. Bergamini, L. H. Marcolino Jr and A. J. G. Zarbin, *Sci. Rep.*, 2016, **6**, 33806.